

hnRNP family protein の機能異常に着目した ALS 病態メカニズムの解明

Altered regulation of hnRNPA1 expression causes ALS- and MSP-linked
cytotoxicity

鈴木宏昌
東京医科大学
薬理学分野

使用ソフト：Microsoft Word

Contents

Introduction.....	3
Materials and Methods.....	4
Results.....	8
Discussion.....	11
References.....	13
Figures.....	18
Abbreviations.....	26

Introduction

Amyotrophic lateral sclerosis (ALS) is a devastating motor neuron specific neurodegenerative disease (1). Approximately 10% of ALS cases occur in a genetically inherited manner (2). Frontotemporal lobar degeneration (FTLD) is the second most common disease with early-onset dementia, characterized by degeneration of the frontal and anterior temporal lobes of cerebral cortices (3).

Missense mutations in multiple heterogeneous nuclear ribonucleoproteins (hnRNPs) including transactive response DNA-binding protein-43 (TDP-43) and fused in sarcoma (FUS) cause familial and sporadic ALS, FTLD, or both. Furthermore, wild-type (wt)-TDP-43 has been found to be a major component of intracellular aggregates in a majority of ALS and in some types of FTLD (4, 5) and FUS has been found to be aggregated in some ALS and FTLD cases without genetic alterations of the *FUS* gene (6, 7). Based on these findings, it has been hypothesized that the gain-of-function and/or loss-of-function of these hnRNPs may be closely linked to the pathogenesis of ALS and FTLD (3, 8). In reality, a number of studies showed that the constitutive overexpression of TDP-43 or FUS, in the presence or the absence of mutations, results in ALS/FTLD phenotypes *in vitro* and *in vivo* (9-14). We also found that low-grade overexpression of wt-TDP-43 or wt-FUS induces neuronal cell death *in vitro* (15-18). In parallel, a number of studies demonstrated that levels of TDP-43 or FUS expression are upregulated in some sporadic ALS and FTLD cases (19-25). It is therefore highly likely that overexpression of TDP-43 and FUS, even in the absence of genetic mutations, may contribute to the onset and the progression of at least some ALS or FTLD cases.

Missense mutations in *HNRNPA1*, the gene encoding heterogeneous nuclear ribonucleoprotein A1 (hnRNPA1), cause ALS and multisystem proteinopathy (MSP) (26). The disease-linked mutations enhance hnRNPA1 fibrillization and recruitment of hnRNPA1 to RNA granules (26). In MSP patients with an hnRNPA1 mutation, hnRNPA1 mislocalizes in the cytoplasm and the nuclear level of hnRNPA1 is decreased in some fibers in muscle. These pathological features are also observed in both familial and sporadic inclusion body myositis cases without the hnRNPA1 mutations (26, 27). Currently, it is not known how the mutations of hnRNPA1 are linked to cytotoxicity and whether these pathological features are causes of, independent co-incidences to, or results of hnRNPA1-linked cytotoxicity.

In this study, we first show that low-grade overexpression of hnRNPA1 causes cell death via the mitochondria apoptosis pathway, mediated by JNK signaling. Second, hnRNPA1 negatively regulates its own mRNA expression by inhibiting splicing of hnRNPA1 pre-mRNA. Given that hnRNPA1 mislocalizes in the cytoplasm and forms aggregation, it is possible that the autoregulation by hnRNPA1 mutant is diminished in pathological condition. Finally, the ALS- and MSP-linked mutations of hnRNPA1 delay protein degradation of hnRNPA1. Taken together, these results suggest that increased protein levels of hnRNPA1, caused by the mutations, cause cytotoxicity.

Materials and Methods

Antibodies and compounds

The following antibodies were purchased from suppliers: hnRNPA1 (4296S), cleaved-caspase-3, cleaved-PARP, GAPDH, Bim, and phosphorylated-JNK, Cell Signaling TECHNOLOGY; TDP-43, ProteinTech Group, Inc; JNK1 and Bcl-xL, Santa Cruz; Horseradish peroxidase (HRP)-conjugated anti-FLAG antibody and actin, Sigma; Xpress, Invitrogen; HRP-conjugated goat anti-rabbit secondary antibody and HRP-conjugated goat anti-mouse secondary antibody, Bio-Rad. Staurosporine and AS601245 were purchased from Calbiochem. Doxycycline was purchased from Clontech.

Plasmid constructs

Human hnRNPA1a cDNA (RefSeq NM_002136.2) was provided by Dr. Naoyuki Kataoka (Kyoto University Graduate School of Medicine). Human hnRNPA1b cDNA (RefSeq NM_031157.2) was provided by Dr. Adrian R. Krainer (Cold Spring Harbor). Human TDP-43 cDNA was provided by Dr. Randal S. Tibbetts (University of Wisconsin). The hnRNPA1a cDNA was subcloned into the pEF1/Myc-His vector (Invitrogen) with a native stop codon to construct non-tagged hnRNPA1a. The FLAG-tagged hnRNPA1a cDNA was subcloned into the pEF1/Myc-His vector and pEF4/His vector (Invitrogen) with a native stop codon to construct FLAG-tagged hnRNPA1a and His-Xpress-FLAG tagged hnRNPA1a, respectively. hnRNPA1a-D262N, -D262V, and - Δ PrLD (Δ prion-like domain, Δ 234-272 in hnRNPA1a) were generated by KOD-Plus-Mutagenesis kit (Toyobo). The FLAG-tagged hnRNPA1a-wt, -D262N, and -D262V cDNA were subcloned into pTRE-Tight vector (Clontech).

Adenoviral vector-mediated expression

The systems of adenovirus expression vectors were purchased from TaKaRa. LacZ, Cre, Cre-TDP-43-wt, and Cre-Bcl-xL adenoviruses were as described previously (15). cDNAs encoding non-tagged hnRNPA1a-wt, -D262N, -D262V, - Δ PrLD, non-tagged hnRNPA1b-wt were inserted into the SmaI site of a cosmid adenoviral vector, pAxCALNLw. In this vector, a stuffer DNA fragment, sandwiched by two loxP sequences, is located just upstream of cDNA and interferes with gene expression. If an adenovirus vector expressing Cre-recombinase is co-introduced into the cells, the stuffer is removed and gene begins to be expressed. All viruses were grown in HEK293 cells and purified by CsCl₂ gradient ultracentrifugation.

Cell culture and transfection

NSC34 cell, a hybrid cell line established from a mouse neuroblastoma cell line and mouse embryo spinal cord cells, was a kind gift from Dr. Neil Cashman (University of Toronto). NSC34, HeLa, and HEK293 cells were grown in Dulbecco's modified Eagle's medium (DMEM), supplemented with 10% of fetal bovine serum (FBS) (Hyclone). HeLa cells, engineered to express a transcription factor rtTA-Advanced (Clontech), were grown in DMEM, supplemented with 10% of FBS (Hyclone) and 100 μ g/mL G418 (Sigma). Transfection was performed using Lipofectamine (Invitrogen)

and PLUS reagent (Invitrogen) under the manufacturer's protocol.

Primary cultured cerebral cortical neurons

Primary cultured cerebral cortical neurons (PCNs), obtained from embryonic day 14 ICR mice, were seeded on poly-l-lysine-coated 96-well plates (Becton Dickinson) at 5×10^4 cells/well or poly-l-lysine-coated 6-well plates (Sumitomo Bakelite) at 1×10^6 cells/well in Neuron medium (Sumitomo Bakelite). Purity of neurons by this method was >98%. PCNs were infected with adenoviruses at the indicated multiplicities of infection (mois) in Neuron medium.

Cell death assay and cell viability assay

Cells, seeded on six-well plates, were incubated with adenovirus-containing media at the indicated moi at 37°C for 1 h with agitation. At 24 h after infection, media of cells were replaced by DMEM with N2 supplement (Invitrogen) to perform lactate dehydrogenase (LDH) release assay as cell death assay. At 24 h after the replacement of media, LDH amounts in the replaced media were measured with an LDH assay kit (Wako). Practically, absorbance (Abs) of the mixtures at 560 nm wavelength was measured by a multilabel reader 2030 ARVOTM X5 (Perkin Elmer). Cell viability was measured by WST-8 cell viability assays. The WST-8 assay, performed using Cell Counting kit-8 (Dojindo), was based on the ability of cells to convert a water-soluble 2-(2-methoxy-4-nitrophenyl)-3-(4-nitrophenyl)-5-(2, 4-disulfophenyl)-2H-tetrazolium monosodium salt into a water-soluble formazan. Cells were treated with WST-8 reagent at 37°C and 450 nm absorbance was measured.

Western blot analysis

Cells were homogenized with a cell lysis buffer [10 mM Tris-HCl (pH 7.4), 1% Triton X-100, 1 mM EDTA, protease inhibitors, phosphatase inhibitors] by a freeze-thaw cycle or solubilized by sonication in a 4% sodium dodecyl sulfate (SDS)-containing sample buffer. The samples in the SDS-containing sample buffer were boiled for 5 min at 95°C, fractionated by SDS-polyacrylamide gel electrophoresis (SDS-PAGE), and blotted onto polyvinylidene fluoride membranes. Immunoreactive bands were detected with ECL Western blotting detection reagents (Amersham Biosciences). Glyceraldehyde 3-phosphate dehydrogenase (GAPDH) or actin was visualized as an internal control.

siRNA-mediated knock-down

siRNAs against hnRNPA1 and non-targeting control siRNA were purchased from RNAi Co., Ltd.. The siRNA sequence for hnRNPA1-#1 and -#2 are 5'-CUUUGGGUUUGUCACAU AUGC -3' and 5'-CAAGAGAUGGCUAGUGCUUCA -3', respectively. siRNAs against TDP-43 (L-012394-00) and negative control (D-001810-10) were purchased from Dharmacon. HeLa cells were transfected using Lipofectamine2000 (Invitrogen) according to the manufacturer's reverse transfection protocol. Briefly, 5×10^4 cells per well on six-well plates were combined with the 5 nM siRNA and Lipofectamine2000 reagent complexes.

hnRNPA1 intron 10 splicing assay

Total RNA was extracted from NSC34 cells that had been introduced

with hnRNPA1a-encoding adenovirus vector together with a reporter vector using the RNeasy Plus mini kit (Qiagen) with DNase treatment (Qiagen). First-strand cDNAs were synthesized from total RNA using Sensescript reverse transcriptase (Qiagen). PCR amplification with KOD-plus-ver. 2 (Toyobo) was performed under denaturation at 98°C for 10 s, annealing at 59°C for 30 s, and elongation at 68°C for 45 s, repeated 30 cycles for hnRNPA1 fragment and 19 cycles for GAPDH. The sequences of forward and reverse primers are as follows: hnRNPA1 fragment, sense: 5'-CTAACACCGAGTTCGTGAAG-3', antisense: 5'-CACCCTGTGCTTGGCTG-3'; GAPDH, sense: 5'-ACCACAGTCCATGCCATCAC-3', antisense: 5'-TCCACCACCCTGTTGCTGTA-3'. The hnRNPA1 forward and reverse primers are located within the *Renilla* luciferase gene and the hnRNPA1 exon11 region, respectively.

Quantitative real-time PCR analysis

Total RNA was extracted from HeLa cells or NSC34 cells infected with indicated adenovirus vectors using RNeasy Plus mini kit (Qiagen) with DNase treatment (Qiagen) or ISOGEN (Wako). Reverse transcription and PCR reactions were performed on an Applied Biosystems StepOnePlus™ Real-Time PCR System (Applied Biosystems) using the Taqman RNA-to-Ct 1-Step Kit (Applied Biosystems). The pairs of primers and the Taqman probes for target mRNAs were designed based on human or mouse mRNA sequences using TaqMan Gene Expression Assays (Applied Biosystems, Assay ID: human hnRNPA1, Hs01656228_s1; human GAPDH, Hs02758991_g1; mouse hnRNPA1, Mm02528230_g1; mouse GAPDH, Mm99999915_g1). The target sequence of human hnRNPA1 and mouse hnRNPA1 probes is located within 5'UTR region of human hnRNPA1 and 3'UTR region of mouse hnRNPA1, respectively, and these probes can detect only endogenous hnRNPA1a and hnRNPA1b mRNA expression. Data analysis was performed using StepOne Software ver. 2.0.2 (Applied Biosystems). Relative mRNA expression was analyzed by the relative standard curve method. Data were normalized to the mRNA expression of *GAPDH*.

Luciferase assay

The luciferase reporter plasmid vector (psiCHECK2) (provided by Dr. Sean P. Ryder, University of Massachusetts Medical School) is a reporter plasmid containing the target sequence cloned into the multiple cloning site located just downstream of the *Renilla* luciferase translational stop codon. The cloned target sequence is transcribed as a part of *Renilla* luciferase mRNA. The firefly luciferase gene, which expresses firefly luciferase under the control of distinct promoter from the *Renilla* luciferase gene, is in tandem inserted downstream of the target sequence to monitor transfection efficiency. 5'UTR, 3'UTR, and intron regions of the human *HNRNPA1* gene were cloned from total RNA or genomic DNA of HeLa and HL60 cells. NSC34 cells, seeded onto 24-well plates at 4×10^4 cells/well, were transfected with the reporter plasmid together with a hnRNPA1a-encoding vector. At 48 h after transfection, luciferase assays were performed with Dual-Luciferase Reporter Assay (Promega). Calculated luciferase activities were normalized by transfection efficiency.

Statistical analysis

All values in the figures are shown as means \pm SD. All experiments that were statistically analyzed were performed with N=3. Statistical analysis was performed with Student's T test. *: $p < 0.05$ n.s.: not significant

Results

Low-grade overexpression of hnRNPA1 induces cell death

The mutations in the prion-like domain of hnRNPA1 cause ALS and MSP (26). We first asked whether the gain-of-function of hnRNPA1 causes cytotoxicity. To address this question, the effect of overexpression of hnRNPA1 on cell viability was examined using hnRNPA1-encoding recombinant adenovirus vectors. The *HNRNPA1* gene has been found to encode two splicing transcripts, a shorter isoform hnRNPA1a (320 a.a.) and a longer isoform hnRNPA1b (372 a.a.). The level of hnRNPA1a expression is 20-times more abundant than that of hnRNPA1b in most tissues (28). Using lactate dehydrogenase (LDH) release cell death assay, we found that increase in expression of hnRNPA1a expression by less than two times over the endogenous level caused cell death in mouse motoneuronal NSC34 cells (Figs. 1a and b, lanes 2-5) and in human adenocarcinoma HeLa cells (Figs. 1c and d) in an expression-level-dependent manner. Performing WST-8 cell viability assay, we also found that overexpression by less than 1.5 times over the endogenous level decreased cell viability of primary cultured cerebral cortical neurons (PCNs) (Figs. 1e and f). Low-grade overexpression of hnRNPA1b, the other isoform of hnRNPA1, also caused cell death (Figs. 1g and h). In contrast, knock-down of endogenous hnRNPA1 expression did not result in any cytotoxicity (Figs. 1i and j). This result suggests that the gain-of-function, but not the loss of function, of hnRNPA1 causes cytotoxicity *in vitro*. Overexpression of TDP-43 downregulated endogenous hnRNPA1a expression (Fig. 1b, lanes 1 and 2) owing to an unknown mechanism.

hnRNPA1 induces cell death via JNK signaling and mitochondria apoptotic pathway

hnRNPA1a-induced cell death was associated with increased cleavage of caspase-3 (Fig. 1b). Co-expression of Bcl-xL completely inhibited hnRNPA1a-induced cell death and reversed the hnRNPA1a-mediated increase in the cleavage of caspase-3 and cleavage of poly (ADP-ribose) polymerase (PARP), one of the caspase substrates (Figs. 2a and b). These results together indicate that hnRNPA1a induces cell death through the mitochondrial apoptotic pathway.

We previously showed that low-grade overexpression of TDP-43 induces cell death via some cell death mediators such as JNK and Bim (15, 16). It was also shown that hnRNPA1 partially colocalizes with TDP-43 in a muscle fiber of MSP patients (26) and TDP-43 binds to hnRNPA1 (29). Based on these findings, it could be hypothesized that there are common downstream mediators for TDP-43- and hnRNPA1-induced cytotoxicity. Therefore, we examined the effect of overexpression of hnRNPA1a on these mediators and found that overexpression of hnRNPA1a did not upregulate Bim expression as TDP-43 did (Fig. 1b). On the other hand, overexpression of hnRNPA1a upregulated JNK phosphorylation, albeit to a smaller extent than TDP-43 did (Fig. 1b). In accordance with the latter finding, a JNK inhibitor AS601245 inhibited hnRNPA1a-induced cell death (Figs. 2c and d). These results suggest that the cell death signaling, triggered by hnRNPA1a, is mediated by JNK and is partially in common with that by TDP-43. We excluded the possibility that TDP-43 is a downstream cell death mediator of hnRNPA1a by confirming that knock-down of endogenous TDP-43 expression did not affect hnRNPA1a-induced cell

death (Figs. 2e and f).

hnRNPA1 downregulates its own mRNA expression

Recent studies have shown that TDP-43 and FUS, belonging to the hnRNP family, autoregulate their own mRNA expression (30–32). We examined whether hnRNPA1 also autoregulates its own mRNA expression. To this end, human hnRNPA1a and hnRNPA1b were overexpressed in NSC34 cells and HeLa cells. In NSC34 cells, overexpression of hnRNPA1a decreased the expression of endogenous hnRNPA1b (long exposure of Fig. 3a, lanes 1 and 2) and overexpression of hnRNPA1b decreased the expression of endogenous hnRNPA1a (Fig. 3a, lanes 1 and 3). It is technically uncertain whether overexpression of hnRNPA1a or hnRNPA1b also decreased the expression of endogenous hnRNPA1a or hnRNPA1b, respectively, because it is impossible to differentiate exogenous and endogenous hnRNPA1a and hnRNPA1b expression. Similarly, in HeLa cells, overexpression of hnRNPA1a or hnRNPA1b reduced the expression of endogenous hnRNPA1b or hnRNPA1a, respectively (Fig. 3b). In agreement, quantitative real time PCR analysis showed that overexpression of hnRNPA1a or hnRNPA1b downregulated endogenous levels of mRNA of hnRNPA1 consisting of both hnRNPA1a and hnRNPA1b in NSC34 cells (Fig. 3c) and HeLa cells (Fig. 3d). A similar result was repeatedly obtained using PCNs (Fig. 3e). These data indicated that hnRNPA1 downregulates its own mRNA expression.

Downregulation of hnRNPA1 mRNA is mediated by inhibition of intron 10 splicing of hnRNPA1 pre-mRNA

The *HNRNPA1* gene is composed of exons 1–11 and introns 1–10 (Fig. 4a). Exon 8 is spliced out in hnRNPA1b. We next examined the molecular mechanism underlying the hnRNPA1 mRNA autoregulation. We first asked whether the mRNA autoregulation of hnRNPA1 mRNA is mediated by the protein-coding region sequence of hnRNPA1. To this end, the non-tagged hnRNPA1a-encoding adenovirus vector was co-infected with the His-Xpress-FLAG-tagged hnRNPA1a (HXF-hnRNPA1a)-encoding adenovirus vector. Both vectors contain only the protein-coding sequence of hnRNPA1. Overexpression of non-tagged hnRNPA1a downregulated endogenous hnRNPA1b whereas it did not affect HXF-hnRNPA1a expression (Fig. 4b). HXF-hnRNPA1a did not decrease the expression of endogenous hnRNPA1 expression probably because of the relatively very low-level expression of HXF-hnRNPA1 (Fig. 4b, upper panel, lanes 1 and 3). Using a dual luciferase assay system, we next examined the involvement of 5' and 3' untranslated regions (UTRs) of hnRNPA1 in the hnRNPA1-mediated downregulation of hnRNPA1 mRNA. In this reporter assay system, a target sequence is cloned into the multiple cloning site (MCS), located just downstream of a *Renilla* luciferase translational stop codon (Fig. 4a, bottom) and the cloned target sequence is transcribed as a part of 3' UTR of *Renilla* luciferase mRNA. We co-transfected a reporter vector that expresses *Renilla* luciferase mRNA fused to the mature whole mRNA of hnRNPA1a consisting of 5'UTR, the coding region of hnRNPA1a, and 3'UTR (Fig. 4a, Mature mRNA of hnRNPA1a), together with the hnRNPA1a-encoding vector into NSC34 cells. We found that overexpression of hnRNPA1a did not reduce luciferase activity (Fig. 4c). Based on these results indicating that the hnRNPA1-mediated downregulation of hnRNPA1 is not

mediated by the exon-derived regions (Figs. 4b and c) and the result indicating that the hnRNPA1-mediated down-regulation is observed in both mouse and human cells (Figs. 3c and d), we hypothesized that hnRNPA1 mRNA autoregulation is mediated by some sequences of hnRNPA1 introns that are conserved between the mouse and the human *HNRNPA1* genes. A BLAST-mediated homology search indicated that the nucleotide sequence of the intron 10 is conserved between mouse and human hnRNPA1 at the highest homology level, prompting us to examine whether the hnRNPA1-induced downregulation of hnRNPA1 mRNA is mediated by the intron 10 sequence. To examine this possibility, we constructed a reporter vector that contains the 3' portion of the exon 10, the intron 10, and the exon 11 of hnRNPA1, inserted downstream of the *Renilla* luciferase region (Fig. 4a, E10/I10/E11). As a putative negative control, we also constructed a reporter vector that contains the exon 10 and the exon 11 downstream of the *Renilla* luciferase region (Fig. 4a, E10/E11). Notably, overexpression of hnRNPA1 significantly decreased luciferase activity in the cells in which the E10/I10/E11 reporter vector was introduced, but not in those in which E10/E11 reporter vector was introduced (Fig. 4d). These results suggest that the hnRNPA1-mediated downregulation of hnRNPA1 is dependent on the intron 10 sequence. Given that most hnRNP family proteins including hnRNPA1 are involved in the regulation of splicing (28, 33), it is possible that hnRNPA1 regulates splicing of the intron 10 of the *HNRNPA1* gene. Performing semi-quantitative PCR analysis using the E10/I10/E11 reporter vector as an artificial hnRNPA1 minigene, we further found that overexpression of hnRNPA1a inhibited the intron 10 splicing (Figs. 4e and f). These results show that hnRNPA1 negatively regulates its own mRNA expression by inhibiting the intron 10 splicing, finally followed by a reduction in mature mRNA.

ALS- and MSP-linked mutations of hnRNPA1 delay protein degradation

We further investigated how the mutations increase cell toxicity. Protein degradation analysis showed that the degradation of hnRNPA1a-D262N and -D262V protein was somewhat delayed as compared with hnRNPA1a-wt, when new-protein synthesis was quenched in a doxycycline-regulated Tet-on system (Fig. 5). This finding suggests that it is likely that the protein levels of hnRNPA1a mutants tend to become a little higher than that of hnRNPA1a-wt, which may contribute to the mild increase in their cell death-inducing activity.

Discussion

In this study, we showed that low-grade overexpression of hnRNPA1 by less than twice the endogenous levels causes cytotoxicity (Fig. 1), and the ALS- and MSP-linked mutations delay protein degradation of hnRNPA1 (Fig. 5). Notably, hnRNPA1 predominantly localizes in the nucleus and overexpression of hnRNPA1 did not result in obvious mislocalization of hnRNPA1 to the cytoplasm in our experimental conditions (data not shown). Consequently, it has been concluded that overexpression of nuclear hnRNPA1 causes cytotoxicity and that cytoplasmic mislocalization and inclusions of hnRNPA1, as observed in clinical samples (26), should be regarded as a result rather than a cause of cytotoxicity. It has been previously hypothesized that the ALS- and MSP-linked mutations increase toxicity by enhancing the aggregation of hnRNPA1 via the C-terminal prion-like domain (26). However, there is no direct evidence indicating that increased aggregation causes cytotoxicity in non-prion neurodegenerative diseases and it is therefore similarly possible that increased aggregation of a responsible protein may be a co-incidence or a result of cytotoxicity. In support, we previously showed that TDP-43 C-terminal fragments that possess pathological features such as hyperphosphorylation and aggregates formation do not induce cytotoxicity (15). Other groups also demonstrated that TDP-43 is toxic without the shift of its localization to the cytoplasm (10, 34-38) and that reducing cytoplasmic aggregation of TDP-43 using synthetic peptides does not prevent cell death (39). In this study, we found that an artificial deletion mutant of hnRNPA1 deficient in the prion-like domain (PrLD) can still induce cell toxicity if it is overexpressed (Figs. 6a and b). This result suggests that the increase in aggregation, caused by the disease-linked mutation, is at least not the sole cause of cytotoxicity.

Increased levels of hnRNPA1 with a disease-linked mutation occurs stabilization of hnRNPA1 protein (Fig. 5). The mechanism underlying the disease-linked mutation-induced stabilization of hnRNPA1 remains to be examined. It was previously shown that a pathological mutation of TDP-43 stabilizes TDP-43 protein and the stability of TDP-43 is correlated to disease onset (34, 40, 41). TDP-43 is cleaved by caspases (15) and the cleavage pattern of TDP-43 determines the speed of clearance and the severity of TDP-43-induced cytotoxicity (42).

hnRNPA1 negatively regulates its own mRNA by attenuating the intron 10 splicing (Figs. 3 and 4). Similarly, other RNA-binding proteins such as TDP-43, FUS, Polypyrimidine tract-binding protein (PTB), Nova, and hnRNPL also possess their own mRNA autoregulation systems (30-32, 43-45). It is highly likely that the levels of these RNA-binding proteins should be tightly regulated to be less than a certain levels because a small excess of protein expression is linked to cytotoxicity or other unfavorable event. Therefore, the impairment of mRNA autoregulation in TDP-43 and FUS may be linked to the pathogenesis of TDP-43 proteinopathy (30-32). Given that hnRNPA1 mislocalizes in the cytoplasm in pathological condition (26), the impairment of mRNA autoregulation of hnRNPA1 by the disease-linked mutations may increase hnRNPA1 expression and contribute to the onset and the progression of hnRNPA1-linked diseases.

It has been reported that MSP with an hnRNPA1 mutation is associated with the TDP-43 pathology (26) and TDP-43 binds to hnRNPA1 (29). Consequently, it

could be assumed that the dysregulation of hnRNPA1 leads to the dysregulation of TDP-43. However, TDP-43 does not appear to be the downstream mediator of hnRNPA1-induced cell death, because knock-down of TDP-43 expression did not affect hnRNPA1a-induced cell death in the employed cell death model (Figs. 2e and f). Thus, the mechanism underlying hnRNPA1-mediated dysregulation of TDP-43 remains to be investigated.

In summary, our results suggest that low-grade overexpression of hnRNPA1 causes cytotoxicity and that the ALS- and MSP-linked mutations of hnRNPA1 may increase cytotoxicity of hnRNPA1 by delaying protein degradation. These results provide a new insight into the pathogenesis of the hnRNPA1-linked ALS and MSP.

References

1. Ferraiuolo, L., Kirby, J., Grierson, A. J., Sendtner, M. and Shaw, P. J. (2011) Molecular pathways of motor neuron injury in amyotrophic lateral sclerosis. *Nat. Rev. Neurol.*, **7**, 616-630.
2. Peters, O. M., Ghasemi, M. and Brown, R. H. Jr. (2015) Emerging mechanisms of molecular pathology in ALS. *J. Clin. Invest.*, **125**, 1767-1779.
3. Halliday, G., Bigio, E.H., Cairns, N.J., Neumann, M., Mackenzie, I.R. and Mann, D.M. (2012) Mechanisms of disease in frontotemporal lobar degeneration: gain of function versus loss of function effects. *Acta Neuropathol.*, **124**, 373-382.
4. Neumann, M., Sampathu, D. M., Kwong, L. K., Truax, A. C., Micsenyi, M. C., Chou, T. T., Bruce, J., Schuck, T., Grossman, M., Clark, C. M. et al. (2006) Ubiquitinated TDP-43 in frontotemporal lobar degeneration and amyotrophic lateral sclerosis. *Science*, **314**, 130-133.
5. Arai, T., Hasegawa, M., Akiyama, H., Ikeda, K., Nonaka, T., Mori, H., Mann, D., Tsuchiya, K., Yoshida, M., Hashizume, Y. et al. (2006) TDP-43 is a component of ubiquitin-positive tau-negative inclusions in frontotemporal lobar degeneration and amyotrophic lateral sclerosis. *Biochem. Biophys. Res. Commun.*, **351**, 602-611.
6. Neumann, M., Rademakers, R., Roeber, S., Baker, M., Kretschmar, H.A. and Mackenzie, I.R. (2009) A new subtype of frontotemporal lobar degeneration with FUS pathology. *Brain*, **132**, 2922-2931.
7. Deng, H.X., Zhai, H., Bigio, E.H., Yan, J., Fecto, F., Ajroud, K., Mishra, M., Ajroud-Driss, S., Heller, S., Sufit, R. et al. (2010) FUS-immunoreactive inclusions are a common feature in sporadic and non-SOD1 familial amyotrophic lateral sclerosis. *Ann. Neurol.*, **67**, 739-748.
8. Lee, E. B., Lee, V. M. and Trojanowski, J. Q. (2011) Gains or losses: molecular mechanisms of TDP43-mediated neurodegeneration. *Nat Rev Neurosci.*, **13**, 38-50.
9. Johnson, B. S., McCaffery, J. M., Lindquist, S. and Gitler, A. D. (2008) A yeast TDP-43 proteinopathy model: Exploring the molecular determinants of TDP-43 aggregation and cellular toxicity. *Proc. Natl. Acad. Sci. U S A.*, **105**, 6439-6444.
10. Liu, Y. C., Chiang, P. M. and Tsai, K. J. (2013) Disease animal models of TDP-43 proteinopathy and their pre-clinical applications. *Int. J. Mol. Sci.*, **14**, 20079-20111.
11. Huang, C., Zhou, H., Tong, J., Chen, H., Liu, Y.J., Wang, D., Wei, X. and Xia, X.G. (2011) FUS transgenic rats develop the phenotypes of amyotrophic lateral sclerosis and frontotemporal lobar degeneration. *PLoS Genet.*, **7**, e1002011.

12. Chen, Y., Yang, M., Deng, J., Chen, X., Ye, Y., Zhu, L., Liu, J., Ye, H., Shen, Y., Li, Y. et al. (2011) Expression of human FUS protein in *Drosophila* leads to progressive neurodegeneration. *Protein Cell*, **2**, 477-486.
13. Vaccaro, A., Tauffenberger, A., Aggad, D., Rouleau, G., Drapeau, P. and Parker, J.A. (2012) Mutant TDP-43 and FUS cause age-dependent paralysis and neurodegeneration in *C. elegans*. *PLoS One*, **7**, e31321.
14. Mitchell, J.C., McGoldrick, P., Vance, C., Hortobagyi, T., Sreedharan, J., Rogelj, B., Tudor, E.L., Smith, B.N., Klasen, C., Miller, C.C. et al. (2013) Overexpression of human wild-type FUS causes progressive motor neuron degeneration in an age- and dose-dependent fashion. *Acta. Neuropathol.*, **125**, 273-288.
15. Suzuki, H., Lee, K. and Matsuoka, M. (2011) TDP-43-induced death is associated with altered regulation of BIM and Bcl-xL and attenuated by caspase-mediated TDP-43 cleavage. *J. Biol. Chem.*, **286**, 13171-13183.
16. Suzuki, H. and Matsuoka, M. (2013) The JNK/c-Jun signaling axis contributes to the TDP-43-induced cell death. *Mol. Cell Biochem.*, **372**, 241-248.
17. Suzuki, H., Shibagaki, Y., Hattori, S. and Matsuoka, M. (2015) Nuclear TDP-43 causes neuronal toxicity by escaping from the inhibitory regulation by hnRNPs. *Hum. Mol. Genet.*, **24**, 1513-1527.
18. Suzuki, H. and Matsuoka, M. (2015) Overexpression of nuclear FUS induces neuronal cell death. *Neuroscience*, **287**, 113-124.
19. Mishra, M., Paunesku, T., Woloschak, G. E., Siddique, T., Zhu, L. J., Lin, S., Greco, K. and Bigio, E. H. (2007) Gene expression analysis of frontotemporal lobar degeneration of the motor neuron disease type with ubiquitinated inclusions. *Acta. Neuropathol.*, **114**, 81-94.
20. Kasai, T., Tokuda, T., Ishigami, N., Sasayama, H., Foulds, P., Mitchell, D. J., Mann, D. M., Allsop, D. and Nakagawa, M. (2009) Increased TDP-43 protein in cerebrospinal fluid of patients with amyotrophic lateral sclerosis. *Acta. Neuropathol.*, **117**, 55-62.
21. Suzuki, M., Mikami, H., Watanabe, T., Yamano, T., Yamazaki, T., Nomura, M., Yasui, K., Ishikawa, H. and Ono, S. (2010) Increased expression of TDP-43 in the skin of amyotrophic lateral sclerosis. *Acta. Neurol. Scand.*, **122**, 367-372.
22. Swarup, V., Phaneuf, D., Dupré, N., Petri, S., Strong, M., Kriz, J. and Julien, J. P. (2011) Deregulation of TDP-43 in amyotrophic lateral sclerosis triggers nuclear factor κ B-mediated pathogenic pathways. *J. Exp. Med.*, **208**, 2429-2447.
23. Verstraete, E., Kuiperij, H. B., van Blitterswijk, M. M., Veldink, J. H., Schelhaas,

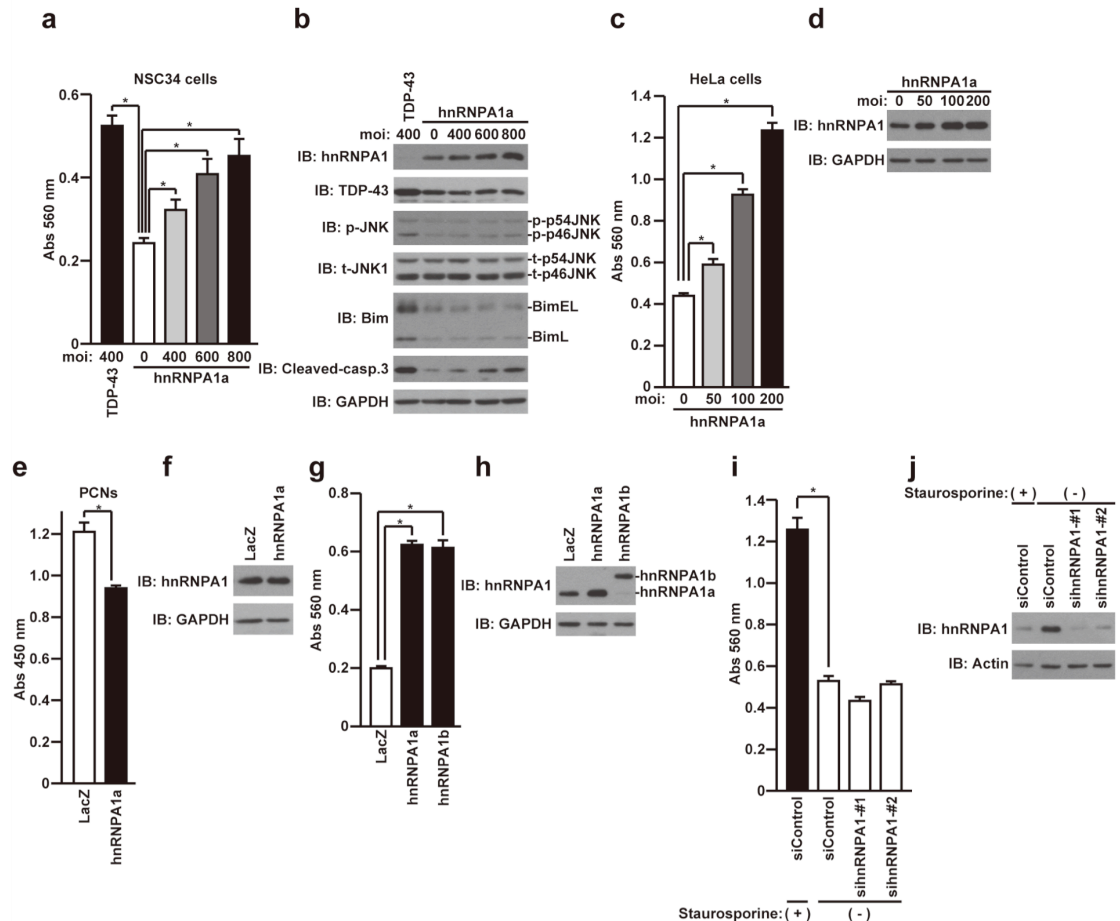
- H. J., van den Berg, L. H. and Verbeek, M. M. (2012) TDP-43 plasma levels are higher in amyotrophic lateral sclerosis. *Amyotroph. Lateral Scler.*, **13**, 446-451.
24. Oketa, Y., Higashida, K., Fukasawa, H., Tsukie, T. and Ono, S. (2013) Abundant FUS-immunoreactive pathology in the skin of sporadic amyotrophic lateral sclerosis. *Acta. Neurol. Scand.*, **128**, 257-264.
 25. Sabatelli, M., Moncada, A., Conte, A., Lattante, S., Marangi, G., Luigetti, M., Lucchini, M., Mirabella, M., Romano, A., Del, Grande, A. et al. (2013) Mutations in the 3' untranslated region of FUS causing FUS overexpression are associated with amyotrophic lateral sclerosis. *Hum. Mol. Genet.*, **22**, 4748-4755.
 26. Kim, H.J., Kim, N.C., Wang, Y.D., Scarborough, E.A., Moore, J., Diaz, Z., MacLea, K.S., Freibaum, B., Li, S., Molliex, A. et al. (2013) Mutations in prion-like domains in hnRNPA2B1 and hnRNPA1 cause multisystem proteinopathy and ALS. *Nature*, **495**, 467-473.
 27. Pinkus, J.L., Amato, A.A., Taylor, J.P. and Greenberg, S.A. (2014) Abnormal distribution of heterogeneous nuclear ribonucleoproteins in sporadic inclusion body myositis. *Neuromuscul. Disord.*, **24**, 611-616.
 28. Jean-Philippe, J., Paz, S. and Caputi, M. (2013) hnRNP A1: the Swiss army knife of gene expression. *Int. J. Mol. Sci.*, **14**, 18999-19024.
 29. Buratti, E., Brindisi, A., Giombi, M., Tisminetzky, S., Ayala, Y.M. and Baralle, F.E. (2005) TDP-43 binds heterogeneous nuclear ribonucleoprotein A/B through its C-terminal tail: an important region for the inhibition of cystic fibrosis transmembrane conductance regulator exon 9 splicing. *J. Biol. Chem.*, **280**, 37572-37584.
 30. Ayala, Y.M., De, Conti, L., Avendaño-Vázquez, S.E., Dhir, A., Romano, M., D'Ambrogio, A., Tollervey, J., Ule, J., Baralle, M., Buratti, E. et al. (2011) TDP-43 regulates its mRNA levels through a negative feedback loop. *EMBO J.*, **30**, 277-288.
 31. Avendaño-Vázquez, S.E., Dhir, A., Bembich, S., Buratti, E., Proudfoot, N. and Baralle, F.E. (2012) Autoregulation of TDP-43 mRNA levels involves interplay between transcription, splicing, and alternative polyA site selection. *Genes Dev.*, **26**, 1679-1684.
 32. Zhou, Y., Liu, S., Liu, G., Oztürk, A. and Hicks, G.G. (2013) ALS-associated FUS mutations result in compromised FUS alternative splicing and autoregulation. *PLoS Genet.*, **9**, e1003895.
 33. Han, S. P., Tang, Y. H. and Smith, R. (2010) Functional diversity of the hnRNPs: past, present and perspectives. *Biochem. J.*, **430**, 379-392.

34. Watanabe, S., Kaneko, K. and Yamanaka, K. (2013) Accelerated disease onset with stabilized familial amyotrophic lateral sclerosis (ALS)-linked mutant TDP-43 proteins. *J. Biol. Chem.*, **288**, 3641-3654.
35. Arnold, E.S., Ling, S.C., Huelga, S.C., Lagier-Tourenne, C., Polymenidou, M., Ditsworth, D., Kordasiewicz, H.B., McAlonis-Downes, M., Platoshyn, O., Parone, P.A. et al. (2013) ALS-linked TDP-43 mutations produce aberrant RNA splicing and adult onset motor neuron disease without aggregation or loss of nuclear TDP-43. *Proc. Natl Acad. Sci. USA.*, **110**, E736–E745.
36. Xu, Y.F., Prudencio, M., Hubbard, J.M., Tong, J., Whitelaw, E.C., Jansen-West, K., Stetler, C., Cao, X., Song, J. and Zhang, Y.J. (2013) The pathological phenotypes of human TDP-43 transgenic mouse models are independent of downregulation of mouse Tdp-43. *PLoS One*, **8**, e69864.
37. Yamashita, M., Nonaka, T., Hirai, S., Miwa, A., Okado, H., Arai, T., Hosokawa, M., Akiyama, H. and Hasegawa, M. (2014) Distinct pathways leading to TDP-43-induced cellular dysfunctions. *Hum. Mol. Genet.*, **23**, 4345–4356.
38. Ash, P.E., Zhang, Y.J., Roberts, C.M., Saldi, T., Hutter, H., Buratti, E., Petrucelli, L. and Link, C.D. (2010) Neurotoxic effects of TDP-43 overexpression in *C. elegans*. *Hum. Mol. Genet.*, **19**, 3206-3218.
39. Liu, R., Yang, G., Nonaka, T., Arai, T., Jia, W. and Cynader, M.S. (2013) Reducing TDP-43 aggregation does not prevent its cytotoxicity. *Acta Neuropathol. Commun.*, **1**, 49.
40. Austin, J. A., Wright, G. S., Watanabe, S., Grossmann, J. G., Antonyuk, S. V., Yamanaka, K. and Hasnain, S. S. (2014) Disease causing mutants of TDP-43 nucleic acid binding domains are resistant to aggregation and have increased stability and half-life. *Proc. Natl. Acad. Sci. U S A.*, **111**, 4309-4314.
41. Ling, S. C., Albuquerque, C. P., Han, J. S., Lagier-Tourenne, C., Tokunaga, S., Zhou, H. and Cleveland, D. W. (2010) ALS-associated mutations in TDP-43 increase its stability and promote TDP-43 complexes with FUS/TLS. *Proc. Natl. Acad. Sci. U S A.*, **107**, 13318-13323.
42. Li, Q., Yokoshi, M., Okada, H. and Kawahara, Y. (2015) The cleavage pattern of TDP-43 determines its rate of clearance and cytotoxicity. *Nat. Commun.*, **6**, 6183.
43. Wollerton, M.C., Gooding, C., Wagner, E.J., Garcia-Blanco, M.A. and Smith, C.W. (2004) Autoregulation of polypyrimidine tract binding protein by alternative splicing leading to nonsense-mediated decay. *Mol. Cell*, **13**, 91–100.
44. Dredge, B.K., Stefani, G., Engelhard, C.C. and Darnell, R.B. (2005) Nova autoregulation reveals dual functions in neuronal splicing. *EMBO J.*, **24**, 1608–1620.

45. Rossbach, O., Hung, L.H., Schreiner, S., Grishina, I., Heiner, M., Hui, J. and Bindereif, A. (2009) Auto- and Cross-Regulation of the hnRNP L Proteins by Alternative Splicing. *Mol. Cell. Biol.*, **29**, 1442-1451.

Figures

Figure 1 Low-grade overexpression of hnRNPA1 induces cell death



(a, b) NSC34 cells, seeded on 6-well plates at 1×10^5 /well, were infected with hnRNPA1a or TDP-43 adenovirus at multiplicities of infection (mois) of 0-800. To keep the total amounts of viruses constant, appropriate amounts of LacZ adenoviruses were added for each infection. All samples were co-infected with Cre-recombinase adenovirus at a moi of 40. At 24 h after infection, media were replaced with DMEM/N2 supplement. At 24 h from the replacement of media, LDH release was measured (a) and immunoblot analysis was performed with indicated antibodies (b). *: $p < 0.05$.

(c, d) HeLa cells, seeded on 6-well plates at 5×10^4 /well, were infected with hnRNPA1a adenovirus at mois of 0-200. To keep the total amounts of viruses constant, appropriate amounts of LacZ adenoviruses were added for each infection. All samples were co-infected with Cre-recombinase adenovirus at a moi of 40. At 24 h after infection, media were replaced with DMEM/N2 supplement. At 24 h from the replacement of media, LDH release was measured (c) and immunoblot analysis was performed with indicated antibodies (d). *: $p < 0.05$.

(e) PCNs, seeded on 96-well plates at 5×10^4 cells/well, were infected with LacZ or hnRNPA1a adenovirus at a moi of 200. All samples were co-infected with

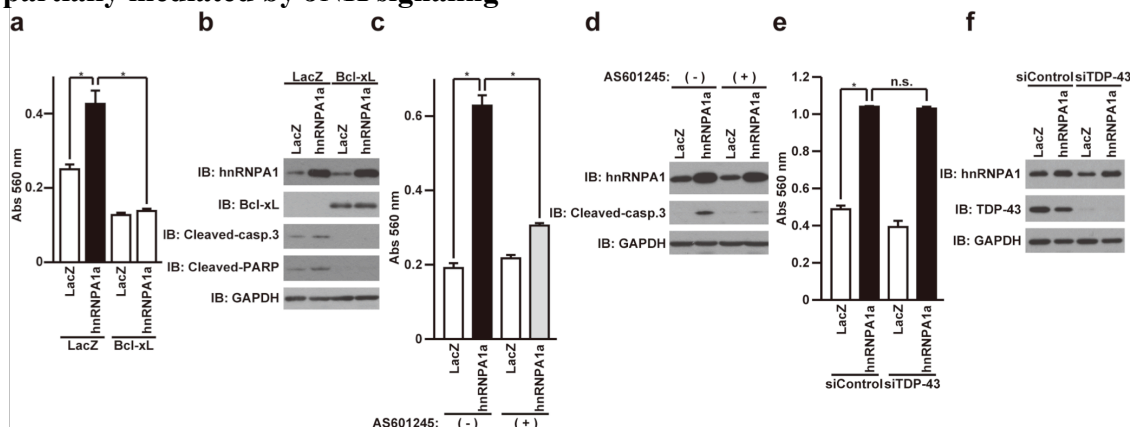
Cre-recombinase adenovirus at a moi of 40. At 72 h after the infection, WST-8 cell viability assay was performed. *: $p < 0.05$.

(f) PCNs, seeded on 6-well plates at 1×10^6 cells/well, were infected with LacZ or hnRNPA1a adenovirus at a moi of 200. All samples were co-infected with Cre-recombinase adenovirus at a moi of 40. At 72 h after the infection, the cell lysates were subject to immunoblot analysis using the indicated antibodies.

(g, h) HeLa cells, seeded on 6-well plates at 5×10^4 /well, were infected with hnRNPA1a or hnRNPA1b adenovirus at moi of 100. All samples were co-infected with Cre-recombinase adenovirus at a moi of 40. At 24 h after infection, media were replaced with DMEM/N2 supplement. At 24 h from the replacement of media, LDH release was measured (g) and immunoblot analysis was performed with indicated antibodies (h). *: $p < 0.05$.

(i, j) HeLa cells, seeded on 6-well plates at 5×10^4 cells/well, were transfected with 5 nM control siRNA, hnRNPA1-#1, or -#2 siRNA using Lipofectamine 2000 reagent. At 48 h after transfection, media were replaced with DMEM/N2 supplement containing or not containing 0.05 μ M staurosporine. At 24 h from the replacement of media, LDH release was measured (i) and immunoblot analysis was performed with indicated antibodies (j). Staurosporine was used as positive control for induction of cell death. The expression of endogenous hnRNPA1 was reduced by treatment with staurosporine, probably because of cleavage or degradation by proteases activated by treatment with staurosporine. *: $p < 0.05$.

Figure 2 hnRNPA1 induces cell death via the mitochondrial apoptosis pathway, partially mediated by JNK signaling

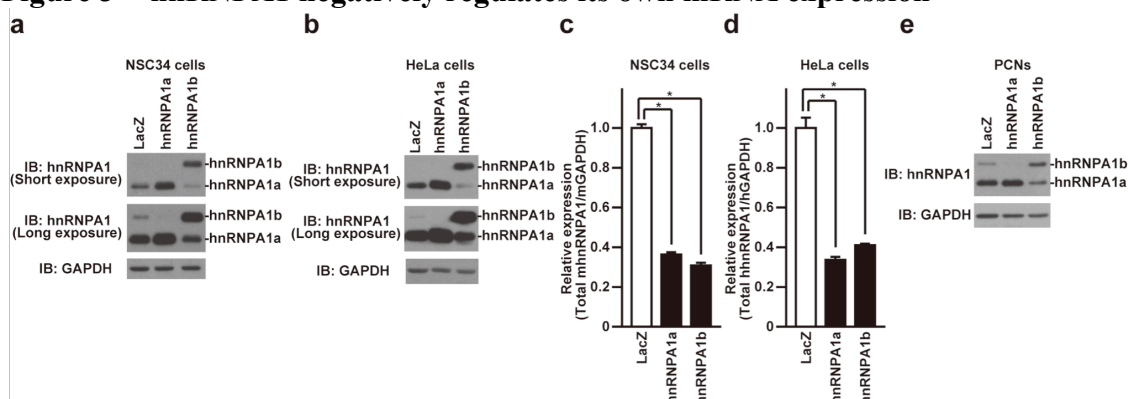


(a, b) NSC34 cells, seeded on 6-well plates at 1×10^5 cells/well, were co-infected with LacZ or hnRNPA1a adenovirus at a moi of 600 in association with LacZ or Bcl-xL adenovirus at a moi of 200. All samples were co-infected with Cre-recombinase adenovirus at a moi of 40. At 24 h after infection, media were replaced with DMEM/N2 supplement. At 24 h from the replacement of media, LDH release was measured (a) and immunoblot analysis was performed with indicated antibodies (b). *: $p < 0.05$.

(c, d) NSC34 cells, seeded on 6-well plates at 1×10^5 cells/well, were infected with LacZ or hnRNPA1a adenovirus at a moi of 800. All samples were co-infected with Cre-recombinase adenovirus at a moi of 40. After infection, cells were co-incubated with or without 2.5 μ M AS601245. At 24 h after infection, media were replaced with DMEM/N2 supplement containing or not containing 2.5 μ M AS601245. At 24 h from the replacement of media, LDH release was measured (c) and immunoblot analysis was performed with indicated antibodies (d). *: $p < 0.05$.

(e, f) HeLa cells, seeded on 6-well plates at 5×10^4 cells/well, were transfected with 5 nM control siRNA or TDP-43 siRNA using Lipofectamine 2000 reagent. At 12 h after transfection, cells were infected with LacZ or hnRNPA1a adenovirus at a moi of 200. All samples were co-infected with Cre-recombinase adenovirus at a moi of 40. At 24 h after infection, media were replaced with DMEM/N2 supplement. At 24 h from the replacement of media, LDH release was measured (e) and immunoblot analysis was performed with indicated antibodies (f). *: $p < 0.05$. n.s.: not significant

Figure 3 hnRNPA1 negatively regulates its own mRNA expression

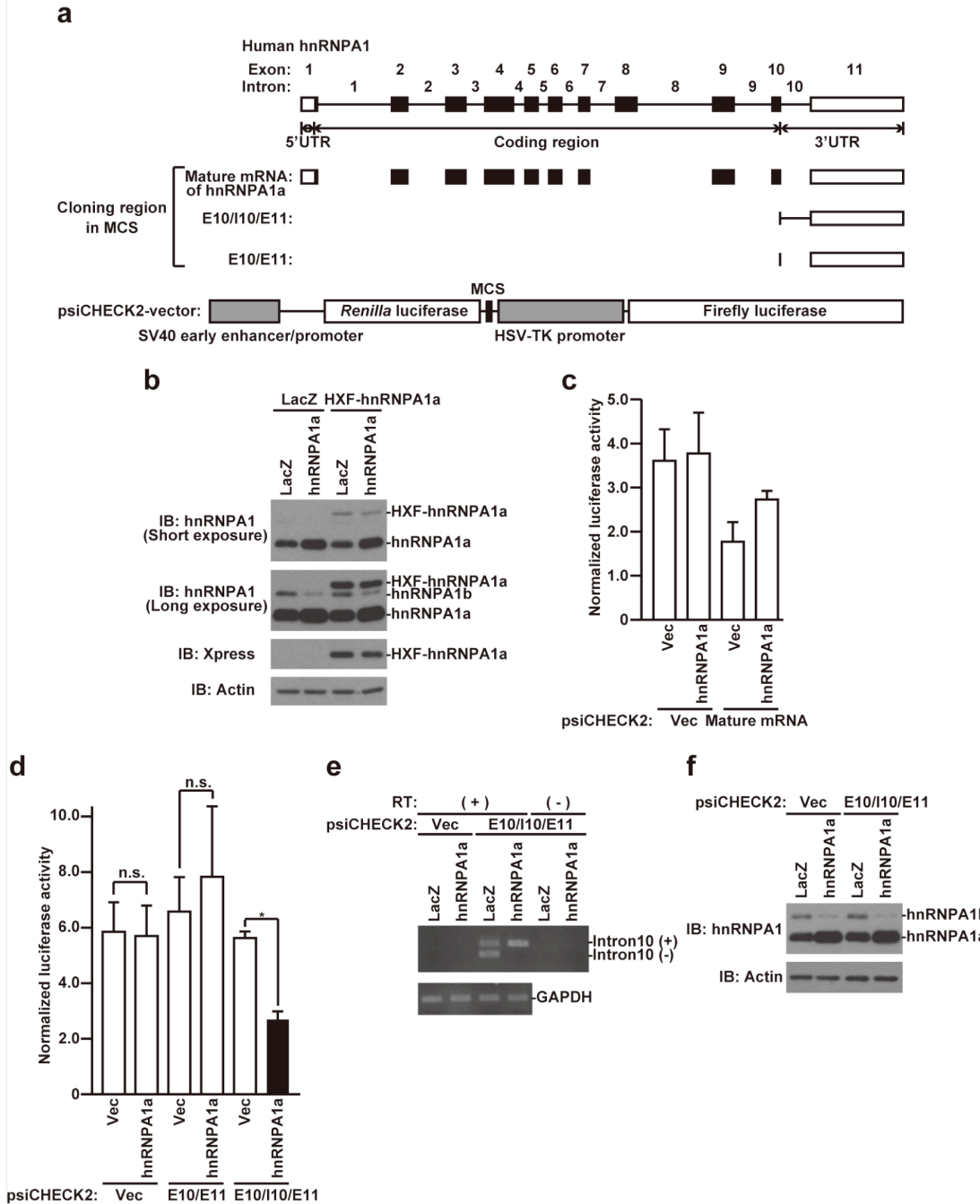


(a, c) NSC34 cells, seeded on six-well plates at 1×10^5 cells/well, were infected with the indicated adenoviruses at a moi of 400. All samples were co-infected with Cre-recombinase adenovirus at a moi of 40. At 48 h after the infection, the cell lysates were subject to immunoblot analysis using the indicated antibodies (a) and quantitative real-time PCR analysis of hnRNPA1 mRNA was performed (c). *: $p < 0.05$.

(b, d) HeLa cells, seeded on six-well plates at 5×10^4 cells/well, were infected with the indicated adenoviruses at a moi of 100. All samples were co-infected with Cre-recombinase adenovirus at a moi of 40. At 48 h after the infection, the cell lysates were subject to immunoblot analysis using the indicated antibodies (b) and quantitative real-time PCR analysis of hnRNPA1 mRNA was performed (d). *: $p < 0.05$.

(e) PCNs, seeded on six-well plates at 1×10^6 cells/well, were infected with the indicated adenoviruses at a moi of 200. All samples were co-infected with Cre-recombinase adenovirus at a moi of 40. At 72 h after the infection, the cell lysates were subject to immunoblot analysis using the indicated antibodies.

Figure 4 Downregulation of hnRNPA1 mRNA is mediated by inhibition of intron10 splicing of hnRNPA1 pre-mRNA



(a) Schematic illustration of the *HNRNPA1* gene and the core of the luciferase reporter vector. The *HNRNPA1* gene is composed of exons 1-11 and introns 1-10. Exon 8 is spliced out in hnRNPA1b. In the luciferase reporter vector, target sequences can be cloned into the multiple cloning site (MCS) located just downstream of the *Renilla* luciferase translational stop codon. The firefly luciferase gene, which expresses firefly luciferase under the control of distinct promoter from the *Renilla* luciferase gene, is in

tandem inserted downstream of the target sequence to monitor transfection efficiency.

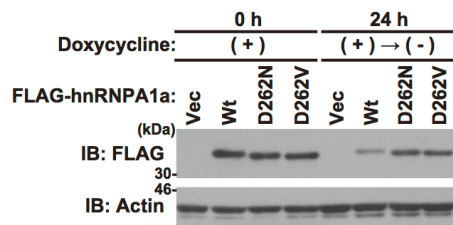
(b) NSC34 cells, seeded on 6-well plates at 1×10^5 cells/well, were co-infected with LacZ or hnRNPA1a adenovirus at a moi of 400 in association with LacZ or His-Xpress-FLAG-tagged hnRNPA1a (HXF-hnRNPA1a) adenovirus at a moi of 200. All samples were co-infected with Cre-recombinase adenovirus at a moi of 40. At 48 h after the infection, the cell lysates were subject to immunoblot analysis using the indicated antibodies

(c) NSC34 cells, seeded on 24-well plates at 4×10^4 cells/well, were transfected with 0.0625 μg /well of the reporter vector in association with 0.025 μg /well of pEF1-Myc/His-vec or pEF1-hnRNPA1a. At 48 h after transfection, luciferase activity was measured by dual-luciferase assays.

(d) NSC34 cells, seeded on 24-well plates at 4×10^4 cells/well, were transfected with 0.0625 μg /well of indicated reporter vector in association with 0.025 μg /well of pEF1-Myc/His-vec or pEF1-hnRNPA1a. At 48 h after transfection, luciferase activity was measured by dual-luciferase assays. *: $p < 0.05$. n.s.: not significant

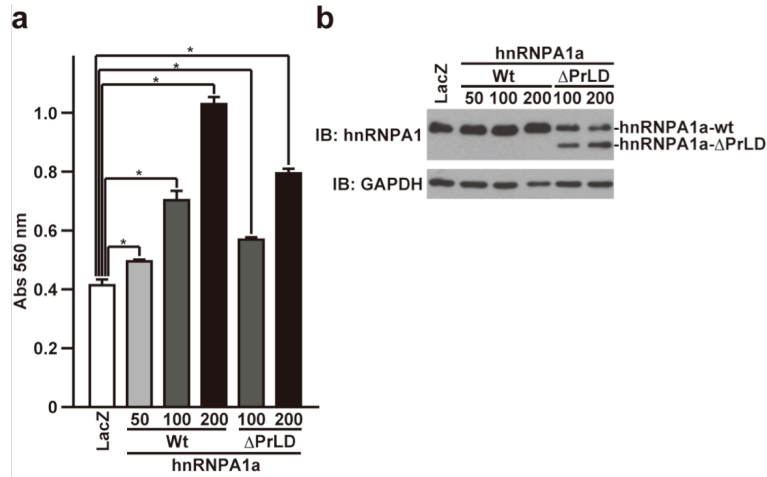
(e, f) NSC34 cells, transiently overexpressed hnRNPA1a by adenoviral infection at a moi of 800 together with psiCHECK2-hnRNPA1-E10/I10/E11 reporter plasmid by transfection, were harvested at 48 h after transfection and the prepared total RNA were used for splicing assays (e). Reverse transcription (RT) (-) was used as negative control for monitoring of PCR amplification from plasmid DNA. All samples were co-infected with Cre-recombinase adenovirus at a moi of 40. intron 10 (+) or (-) indicated the amplicon that include or does not include intron 10 region, respectively. The cell lysates were subject to immunoblot analysis using the indicated antibodies (f).

Figure 5 ALS- and MSP-linked mutations of hnRNPA1 delay protein degradation



HeLa cells, engineered to express a transcription factor rtTA-Advanced, were transfected with pTRE-Tight-FLAG-hnRNPA1a-wt, -D262N, or -D262V. At 24 h after the transfection, the cells were co-incubated with 0.02 $\mu\text{g}/\text{mL}$ doxycycline for 24 h. At 24 h from the start of co-incubation, doxycycline was removed. At 24 h after the removal of doxycycline, the cells were harvested for immunoblot analysis with indicated antibodies.

Figure 6 hnRNPA1 induces cell death independently of the prion-like domain (PrLD)



(a, b) HeLa cells, seeded on 6-well plates at 5×10^4 /well, were infected with hnRNPA1a-wt or - Δ PrLD adenovirus at mois of 50-200. To keep the total amounts of viruses constant, appropriate amounts of LacZ adenoviruses were added for each infection. All samples were co-infected with Cre-recombinase adenovirus at a moi of 40. At 24 h after infection, media were replaced with DMEM/N2 supplement. At 24 h from the replacement of media, LDH release was measured (a) and immunoblot analysis was performed with indicated antibodies (b). *: $p < 0.05$.

Abbreviations

ALS, amyotrophic lateral sclerosis; FTLD, frontotemporal lobar degeneration; FUS, fused in sarcoma; GAPDH, glyceraldehyde-3-phosphate dehydrogenase; hnRNP, heterogeneous nuclear ribonucleoprotein; LDH, lactate dehydrogenase; MSP, multisystem proteinopathy; PCNs, primary cultured cerebral cortical neurons; PrLD, prion-like domain; TDP-43, transactive response DNA-binding protein-43